4594 *Inorg. Chem.* **2010**, *49*, 4594–4598
DOI: 10.1021/ic100164k

Inorganic Chemistry
Article

Structure and Magnetic Field-Induced Transition in a One-Dimensional Hybrid Inorganic−Organic Chain System, Co_2(4,4′-bpy)(tfhba)$_2$·4,4′-bpy (4,4′-bpy = 4,4′-Bipyridine; tfhba = 2,3,5,6-Tetrafluoro-4-hydroxybenzoate)

Zeric Hulvey,*,† Brent C. Melot,† and Anthony K. Cheetham*,‡

†*Materials Research Laboratory, University of California, Santa Barbara, California 93106-5121, and* ‡*Department of Materials Science and Metallurgy, University of Cambridge, Pembroke Street, Cambridge CB2 3QZ, U.K.*

Received January 26, 2010

Two isostructural hybrid inorganic−organic frameworks, M_2(4,4′-bpy)(tfhba)$_2$·4,4′-bpy, (M = Co (**1**), Zn (**2**); 4,4′-bpy = 4,4′-bipyridine; tfhba = 2,3,5,6-tetrafluoro-4-hydroxybenzoate) have been synthesized and their structures elucidated using single crystal X-ray diffraction. These materials are the first hybrid structures synthesized using the tfhba ligand. They contain a one-dimensional chain of corner-sharing MO_4N trigonal bipyramids that has not been observed to date for Co^{2+} units. The magnetic properties of **1** have been investigated and indicate ferromagnetic ordering along the chains, with weak antiferromagnetic interactions between them. Overall the system is antiferromagnetic with a Néel temperature of 3 K, but undergoes a field-induced magnetic phase transition at 3 kOe.

Introduction

Hybrid inorganic−organic materials have gained significant attention over the past decade for their increasingly wide range of applications. Most of this attention has focused on highly porous coordination polymers (also known as Metal-Organic Frameworks, MOFs) and their uses in gas storage and catalysis.[1,2] However, dense hybrid materials, especially those with extended metal−oxygen−metal (M-O-M) connectivity, are beginning to receive attention because of their interesting magnetic, optical, and electronic properties.[3,4] The range of hybrid structures that have shown noteworthy magnetic properties is very diverse and is typically marked by the degree and manifestation of inorganic connectivity between the cations in the structure. While there are examples of magnetic materials containing only isolated cations or clusters of metal centers connected through either carboxylate or other functional groups (0-D M-O-M connectivity), structures containing inorganic chains, layers, or 3-D frameworks more commonly display interesting magnetic behavior.[5−8]

The present work involves the synthesis of hybrid structures using perfluorinated carboxylates, which to date have not been extensively investigated. We have previously shown that perfluorinated dicarboxylates, when used in combination with bipyridines and other small basic ligands, can be incorporated into hybrid frameworks with a diverse range of dimensionalities and structure types.[9−12] Here we report two isostructural materials with 1-D M-O-M connectivity, M_2(4,4′-bpy)(tfhba)$_2$·4,4′-bpy, (M = Co (**1**), Zn (**2**); 4,4′-bpy = 4,4′-bipyridine; tfhba = 2,3,5,6-tetrafluoro-4-hydroxybenzoate). These materials are the first hybrid structures reported using the tfhba ligand. The structure consists of infinite chains of corner-sharing MO_4N trigonal bipyramids connected in one direction by bridging 4,4′-bpy ligands and another by bridging tfhba ligands. Chains of corner-sharing trigonal bipyramidal units are uncommon in the solid state and, to our knowledge, have not been reported for Co^{2+} metal centers. Here we report on the structure and magnetic properties of compounds **1** and **2**.

*To whom correspondence should be addressed. E-mail: zhulvey@chem.ucsb.edu (Z.H.), akc30@cam.ac.uk (A.K.C.).

(1) Kitagawa, S.; Kitaura, R.; Noro, S. *Angew. Chem., Int. Ed.* **2004**, *43*, 2334–2375.
(2) Férey, G. *Chem. Soc. Rev.* **2008**, *37*, 191–214.
(3) Cheetham, A. K.; Rao, C. N. R. *Science* **2007**, *318*, 58–59.
(4) Rao, C. N. R.; Cheetham, A. K.; Thirumurugan, A. *J. Phys.: Condens. Matter* **2008**, *20*, 083202.
(5) Kurmoo, M. *Chem. Soc. Rev.* **2009**, *38*, 1353–1379, and references therein.
(6) Liu, T.; Zhang, Y.; Wang, Z.; Gao, S. *Inorg. Chem.* **2006**, *45*, 2782.
(7) Manna, S. C.; Zangrando, E.; Ribas, J.; Chaudhuri, N. R. *Dalton Trans.* **2007**, 1383.
(8) Feller, R. K.; Melot, B. C.; Forster, P. M.; Cheetham, A. K. *J. Mater. Chem.* **2009**, *19*, 2604.
(9) Hulvey, Z.; Wragg, D. S.; Lin, Z.; Morris, R. E.; Cheetham, A. K. *Dalton Trans.* **2009**, 1131–1135.
(10) Hulvey, Z.; Falcao, E. H. L.; Eckert, J.; Cheetham, A. K. *J. Mater. Chem.* **2009**, *19*, 4307–4309.
(11) Hulvey, Z.; Ayala, E.; Furman, J. D.; Forster, P. M.; Cheetham, A. K. *Cryst. Growth Des.* **2009**, *9*, 4759–4765.
(12) Hulvey, Z.; Ayala, E.; Cheetham, A. K. *Z. Anorg. Allg. Chem.* **2009**, *635*, 1753–1757.

 Published on Web 04/20/2010

Table 1. Crystal Data and Refinement Parameters for **1** and **2**

	1	**2**
formula	$CoC_{17}H_8F_4N_2O_3$	$ZnC_{17}H_8F_4N_2O_3$
molecular weight	423.18	429.62
crystal system	orthorhombic	orthorhombic
space group	*Pmna*	*Pmna*
a/Å	26.271(4)	26.376(3)
b/Å	8.9909(12)	8.9842(10)
c/Å	6.4018(9)	6.3964(7)
V/Å^3	1512.1(4)	1515.8(3)
Z	4	4
ρ/g cm^{-3}	1.859	1.883
μ/mm^{-1}	1.204	1.690
2θ range collected	5.54−49.42°	3.08−50.70°
data/restraints/ parameters	1318/0/133	1430/0/134
R_{int}	0.2195	0.1175
R_1, wR_2 ($I > 2\sigma(I)$)	0.0586, 0.1231	0.0459, 0.1032
R (all data)	0.1077, 0.1402	0.0772, 0.1126

Experimental Section

Synthesis. All reagents were used as received from Aldrich. Syntheses were carried out in Parr Teflon-lined stainless steel autoclaves under autogenous pressure. Purple plates of **1** were obtained from the reaction of $CoCl_2 \cdot 6H_2O$ (0.049 g, 0.20 mmol), H_2-tfhba (0.044 g, 0.20 mmol), and 4,4′-bipyridine (0.015 g, 0.10 mmol) in a mixture of 2 mL of water and 1 mL of ethanol at 100 °C for 20 h. After cooling to room temperature, the crystals were filtered and washed with water and acetone (yield: 52%). Anal. found (wt %): C, 47.9; H, 1.99; N, 6.62. Calculated (wt %): C, 48.3; H, 1.91; N, 6.62. Colorless blocks of **2** were obtained in a similar reaction using $Zn(CH_3CO_2)_2 \cdot 2H_2O$ as the metal salt in 3 mL of water (yield: 63%). Anal. found (wt %): C, 47.5; H, 1.93; N, 6.54. Calculated (wt %): C, 47.5; H, 1.88; N, 6.52.

Structure Determination. Suitable single crystals were selected under a polarizing microscope and glued to a glass fiber. Crystal structure determination by X-ray diffraction (XRD) was performed on a Siemens SMART-CCD diffractometer equipped with a normal focus, 2.4 kW sealed tube X-ray source (Mo Kα radiation, $\lambda = 0.71073$ Å) operating at 45 kV and 35 mA. A hemisphere of intensity data was collected at room temperature. Absorption corrections were made using SADABS.[13] The structures were solved by direct methods and difference Fourier synthesis and were refined against $|F|^2$ using the SHELXTL software package.[14] Details of structure determinations are shown in Table 1. The extinction coefficients refined to within three esd's of zero and were therefore removed from the final refinements. Non-hydrogen atoms were refined anisotropically, and hydrogen atoms were refined isotropically, with thermal parameters equal to 1.2 times those of the respective mother atoms. All hydrogen atoms were found in the Fourier difference map and restrained to chemically reasonable positions.

Magnetic and Specific Heat Measurements. The temperature dependence of the alternating current (AC) and direct current (DC) magnetization was measured on well-ground single crystals of **1** using a Quantum Design MPMS 5XL SQUID magnetometer. Powders were preferred for magnetization measurements since a single crystal of sufficient size and quality could not be obtained. Specific heat data were collected by mixing the cobalt title compound with equal parts by mass of powdered Ag and pressing into a pellet to improve thermal coupling. Measurements were done using a semiadiabatic technique as implemented in a Quantum Design Physical Property Measurement System (PPMS) under zero external magnetic field, as well as under a 10 kOe field. The contribution from Ag was measured separately and subtracted. The specific heat of the Zn analogue was also measured so that the lattice contribution could be subtracted and a more accurate estimation of the magnetic contribution to the specific heat could be obtained.

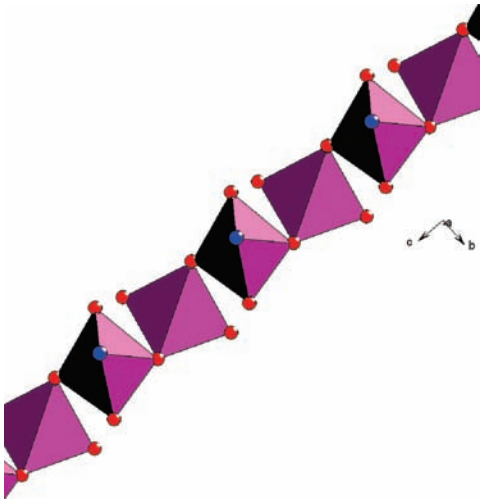

Figure 1. One-dimensional chain of MO_4N trigonal bipyramids in **1** and **2**.

Results and Discussion

Structure of 1 and 2. Compounds **1** and **2** are isostructural and have a three-dimensional structure containing one-dimensional chains of corner-sharing MO_4N trigonal bipyramids which are connected in one direction by bridging 4,4′-bpy ligands and in another by bridging tfhba ligands. It is an I^1O^2 system according to the nomenclature of Cheetham et al.[15] The single unique metal atom is bound to one nitrogen atom from one end of the 4,4′-bpy ligand and four oxygen atoms from four different tfhba ligands. The two axial oxygen atoms are from carboxylate groups, and the two equatorial oxygen atoms are from hydroxyl groups. Each hydroxyl group is bound to two metal atoms, forming an infinite chain of metal−oxygen−metal connectivity down the *c*-axis (Figure 1). To the best of our knowledge, this infinite chain of Co^{2+} trigonal bipyramids is unprecedented in hybrid frameworks. All of the tfhba ligands lie nearly perpendicular to the chain, forming a rather dense layer in the *bc* plane. These layers are pillared in the *a* direction by the 4,4′-bpy ligands (Figure 2), forming the overall three-dimensional grid-like structure with large cavities measuring approximately 8.0 Å × 8.4 Å. An uncoordinated 4,4′-bpy molecule fills the cavity, packing in the same plane as the coordinated 4,4′-bpy molecules around it, so there is no accessible void space.

Thermal Stability. Thermogravimetric analysis (TGA) was performed on a Mettler 851eTG/sDTA to investigate the possibility of removing the guest 4,4′-bpy molecule without decomposing the framework structure. Compounds **1** and **2** are stable to relatively high temperatures, and both TGA data and the corresponding high temperature powder XRD studies indicate that the guest 4,4′-bpy molecules cannot be removed thermally. Once mass loss

(13) Sheldrick, G. M. *SADABS User Guide*; University of Göttingen: Göttingen, Germany, 1995.

(14) Sheldrick, G. M. *SHELXTL-97. A Program for Crystal Structure Determination*, version 5.1; University of Göttingen: Göttingen, Germany, 1995.

(15) Cheetham, A. K.; Rao, C. N. R.; Feller, R. K. *Chem. Commun.* **2006**, 4780–4795.

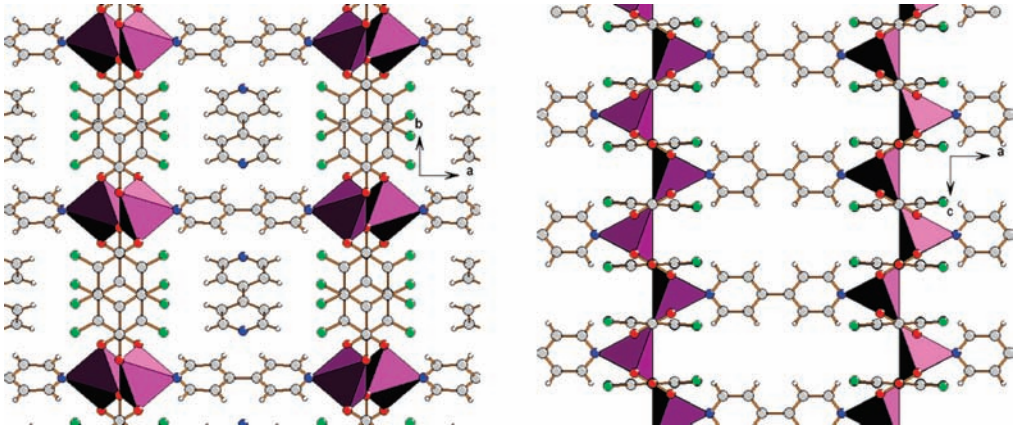

Figure 2. Structure of **1** and **2**; viewed down *c*-axis including uncoordinated 4,4′-bpy molecules (left), and down *b*-axis with uncoordinated 4,4′-bpy molecules not shown (right).

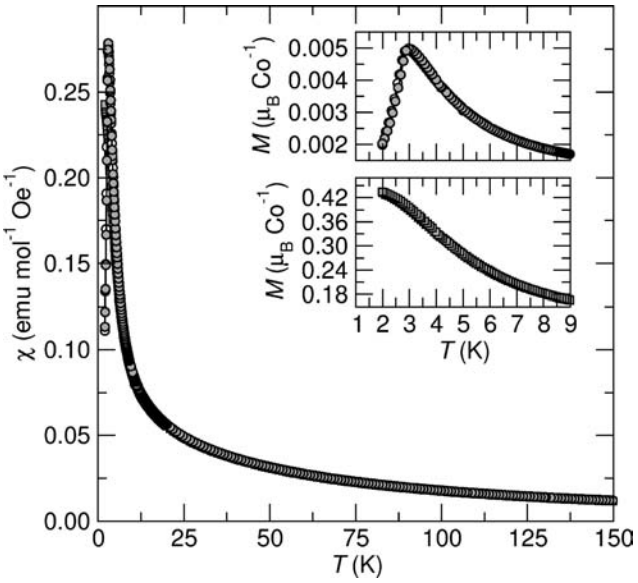

Figure 3. Temperature dependence of the magnetic susceptibility for **1** in 100 Oe (circles) and 10 kOe (squares) where the unfilled symbols are the zero field cooled data and the filled symbols are field cooled. The insets are provided to emphasize the difference in the ordering behavior in 100 Oe (top) and 10 kOe (bottom).

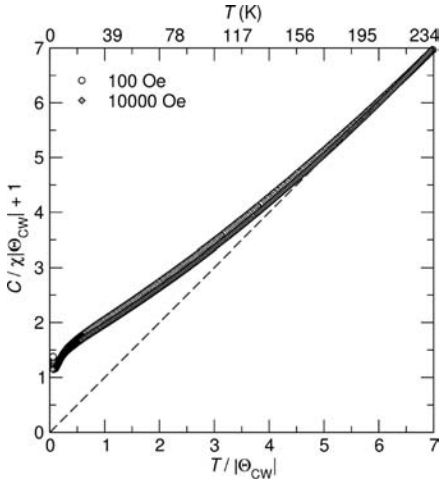

Figure 4. Inverse susceptibility for **1** collected in a field of (a) 100 Oe and (b) 10 kOe normalized by the fit to the Curie−Weiss equation at high temperatures.

begins (270 °C for **1**, 220 °C for **2**), the structure steadily decomposes to give an amorphous material. This resistance to removal is not necessarily surprising when considering the environment of the guest molecule. It is wedged at an angle such that it lies in the same plane as the coordinated 4,4′-bpy molecules, and the nitrogen atoms at both ends are held in place by a hydrogen bonding interaction with two hydrogen atoms from these neighboring 4,4′-bpy ligands (C−H···N distance 2.49 Å). There also appears to be a $\pi-\pi$ stacking interaction between each uncoordinated 4,4′-bpy molecule to the one below it, as they pack in a columnar manner down the *c*-axis with a ring−ring distance of 3.77 Å.

Magnetic Properties. The temperature dependence of the magnetic susceptibility for **1** is shown in Figure 3. A sharp cusp, indicative of antiferromagnetic ordering, is observed around 3 K when the sample is cooled in a field of 100 Oe (Figure 3 top inset). Interestingly, the cusp begins to be suppressed and more closely resembles the plateau-like behavior of ferromagnetic ordering in a field of 10 kOe (Figure 3 bottom inset).

The high temperature region (200 to 300 K) of the inverse susceptibility was fit to the Curie−Weiss equation, $C/(T - \Theta_{CW})$, to obtain the effective moment (μ_{eff}) from the Curie constant and the Curie−Weiss ordering temperature, Θ_{CW}. A Curie−Weiss theta of +39 K and an effective moment of 3.40 μ_B per Co were extracted from the 10 kOe data with essentially the same result being obtained from the 100 Oe data. The effective moment is slightly smaller than the expected spin-only value of 3.87 μ_B for a single high spin Co^{2+} ($S = 3/2$) in a trigonal bipyramidal coordination environment.

The field cooled (FC) susceptibility, scaled using the values of C and Θ_{CW} from the fit to the inverse susceptibility, is shown in Figure 4. The scaling is performed by plotting $C/(\chi|\Theta_{CW}|) + 1$ as a function of $T/|\Theta_{CW}|$, for which Curie−Weiss behavior should yield a straight line through the origin (indicated by the dashed line) for a positive value of Θ_{CW}. Plotting in this manner emphasizes deviations from purely Curie−Weiss behavior. The usefulness of this style of scaling has been discussed in detail elsewhere.[16] It can be

(16) Melot, B. C.; Drewes, J. E.; Seshadri, R.; Ramirez, A. P. *J. Phys.: Condens. Matter* **2009**, *21*, 216007.

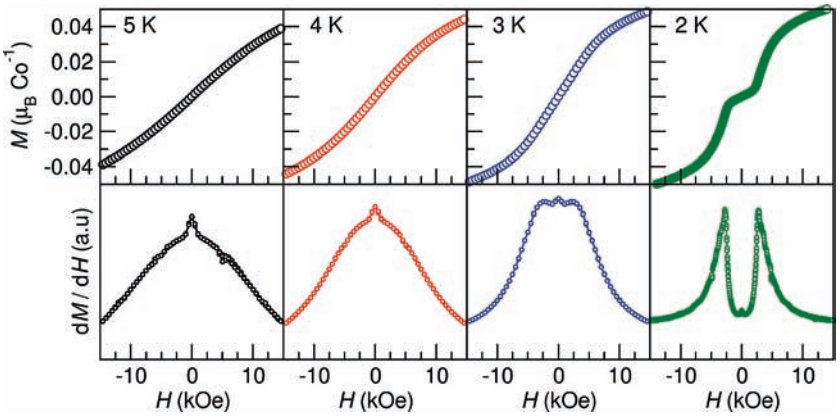

Figure 5. Isothermal magnetic susceptibility (top panel) of **1** and the derivative of the magnetization as a function of field (bottom panel) at various temperatures. A field induced magnetic transition evolves below the magnetic ordering temperature.

seen in Figure 4 that in large as well as small external fields the susceptibility begins to deviate from Curie−Weiss behavior well above the ordering temperature of 3 K. Given the one-dimensional nature of the magnetic interactions, the positive sign of Θ_{CW} most likely indicates that neighboring cobalt ions along the length of each chain, which should be expected to be the dominant magnetic interaction, order ferromagnetically with respect to each other. The positive deviations from the Curie−Weiss law in Figure 4 can be attributed to short-range antiferromagnetic correlations which develop above the ordering temperature and may indicate antiferromagnetic order between the chains.

The large disparity between the Curie−Weiss constant and T_N ($\Theta_{CW}/T_N \sim 13$) is likely a result of frustration because of the large number of exchange pathways that coexist within the crystal structure. Along the length of the chain there are two different exchange pathways, one of the type Co−O−Co (with an angle of 125.9°) and the other of the type Co−O−C−O−Co. There are also two exchange pathways between the chains, mediated by the two different ligands (Co−Co distances through tfhba and 4,4′-bpy ligands 9.0 Å and 11.3 Å, respectively). The closest analogy that we can find to the magnetic structure of the title compound is the system $CsCoCl_3 \cdot 2H_2O$.[17] In the latter case the structure comprises chains of corner-sharing $CoCl_4O_2$ octahedra with a bridging Co−Cl−Co angle of 127.5°. Unlike the cobalt title compound, **1**, the chains appear to be antiferromagnetically ordered in the case of $CsCoCl_3 \cdot 2H_2O$.

To further probe the field dependence of the magnetism, isothermal magnetization curves were collected at several points around the ordering temperature (Figure 5). Starting around 3 K, a field-induced magnetic transition is observed in fields larger than 3 kOe, the details of which can be seen more clearly by examining the derivative of the magnetization (bottom panel of Figure 5). Such behavior reinforces the idea that both ferromagnetic and antiferromagnetic correlations are present in and between the chains, respectively, and that the presence of large external fields suppresses the antiferromagnetic correlations.

The temperature dependence of the specific heat is shown in Figure 6(a). In the absence of an external magnetic field, a sharp anomaly is found at the magnetic ordering temperature of 3 K. When an external field of 10 kOe is applied, the ordering peak is suppressed, but a new bump is found to develop above 3 K. This reflects the release of entropy at temperatures above the magnetic ordering transition, and may be the result of short-range correlations developing in the presence of the field. Figure 6(a) also shows $\partial(\chi T)/\partial T$. Fisher has shown that $\partial(\chi T)/\partial T$ is proportional to the specific heat and true three-dimensional ordering of the spins should be mirrored in both the Fisher specific heat as well as the heat capacity, as shown in Figure 6(a).[18,19] Integration of the magnetic contribution to the specific heat (Figure 6(b)) gives an entropy of 3.3 J mol^{-1} K^{-1} both in the presence and absence of the field and corresponds to 29% of the expected 11.52 J mol^{-1} K^{-1} for $S = 3/2$ Co^{2+}.

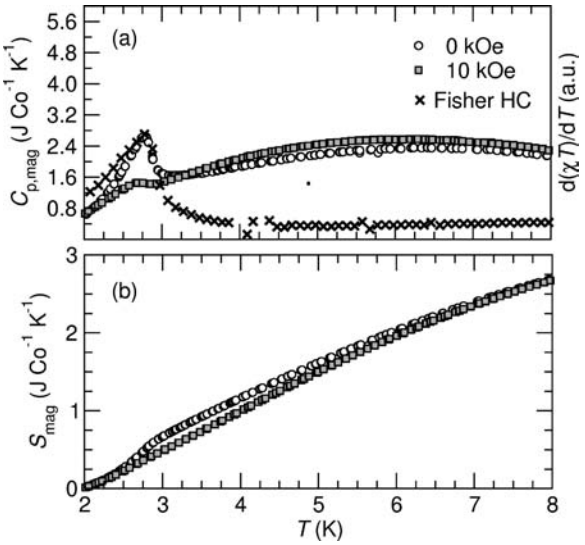

Figure 6. Magnetic specific heat of **1** as a function of temperature and field compared to the Fisher specific heat as described in the text (top) and entropy associated with the magnetic ordering transition in **1** (bottom).

Conclusion

We have isolated and characterized the first hybrid framework structures containing the tfhba ligand. While Zn^{2+}

(17) Herweijer, A.; de Jonge, W. J. M.; Botterman, A. C.; Bongaarts, A. L. M.; Cowen, J. A. *Phys. Rev. B* **1972**, *5*, 4618–4630.

(18) Cage, B.; Nguyen, P.; Dalal, N. *Solid State Commun.* **2001**, *119*, 597–601.

(19) Fisher, M. E. *Proc. R. Soc. A* **1960**, *254*, 66–85.

commonly exhibits the trigonal bipyramidal coordination environment seen in the title structures, Co^{2+} typically prefers octahedral or tetrahedral coordination in hybrid materials, and examples of trigonal bipyramidal coordination are less common.[20−22] The manifestation of the Co^{2+} polyhedra into an infinite chain in **1** is unprecedented and gives rise to both ferromagnetic and antiferromagnetic interactions in its structure.

(20) Zeng, M.-H.; Gao, S.; Chen, X.-M. *Inorg. Chem. Commun.* **2004**, *7*, 864–867.
(21) Fu, S.-J.; Cheng, C.-Y.; Lin, K.-J. *Cryst. Growth Des.* **2007**, *7*, 1381–1384.
(22) Cave, D.; Gascon, J.-M.; Bond, A. D.; Teat, S. J.; Wood, P. T. *Chem. Commun.* **2002**, 1050–1051.

Acknowledgment. We thank Ram Seshadri and Daniel Shoemaker for valuable discussions, and Guang Wu for assistance with XRD experiments. This work was supported by the U.S. Department of Energy (DE-FC36-50GO15004) and made use of the MRL Central Facilities supported by the National Science Foundation (DMR05-20415). B.C.M. is supported by a Career Award to Ram Seshadri (DMR04-49354), and A.K.C. is supported by the European Research Council.

Supporting Information Available: Tables of further crystallographic data and CIF files, and thermogravimetric analysis data. This material is available free of charge via the Internet at http://pubs.acs.org.